A bilateral comparison between LNHB and PTB to determine the activity concentration of the same ^{125}I solution

Karsten Kossert, Christophe Bobin, Vanessa Chisté, Carole Fréchou, Valérie Lourenço, Ole Nähle, Benoit Sabot, Cheick Thiam

A bilateral comparison between LNHB and PTB to determine the activity concentration of the same ^{125}I solution

Karsten Kossert[1*], Christophe Bobin[2], Vanessa Chisté[2], Carole Fréchou[2], Ole Nähle[1], Valérie Lourenço[2] Benoit Sabot[2], Cheick Thiam[2]

[1]*Physikalisch-Technische Bundesanstalt (PTB), Bundesallee 100, 38116 Braunschweig, Germany*

[2]*Université Paris-Saclay, CEA, List, Laboratoire National Henri Becquerel (LNE-LNHB), F-91120 Palaiseau, France*

[*]Corresponding author's e-mail: karsten.kossert@ptb.de

Abstract

A bilateral comparison to determine the activity concentration of the same ^{125}I solution was organized. As electron-capture radionuclide with a rather high atomic number, ^{125}I must be regarded as difficult to measure. The situation is partly exacerbated by the fact that some established standardization methods, like photon-photon coincidence counting, can no longer be applied due to the unavailability of appropriate equipment and expertise.

One aim of this work is to compare modern liquid scintillation counting methods for the standardization of ^{125}I. Both participating metrology institutes have used their custom-built triple-to-double-coincidence ratio (TDCR) counters and the determined activity concentrations are in excellent agreement even though the ways to analyze the data and to compute counting efficiencies were widely independent. The results also agree with the outcome of 4π-γ counting that was carried out at LNHB.

In both laboratories, the measurements were complemented by measurements with several secondary standardization methods which even allow to establish a link to the CCRI(II)-K2.I-125(2) comparison started in 2004. A good agreement between the TDCR results and the key comparison reference value of the 2004 comparison was obtained.

Keywords: ^{125}I; international comparison; activity standardization; liquid scintillation counting; TDCR, 4π-γ counting

1. Introduction

Due to its chemical and physical properties, ^{125}I is suitable for in vivo imaging and various cancer therapies, the most commonly used being brachytherapy for the treatment of different types of tumors (see, e.g., Huang, 2019; Wei et al., 2021). Activity standards are required for calibration purposes, e.g., in medicine, research, and radiation protection.

Iodine-125 decays by electron-capture (EC) to an excited level of ^{125}Te which has a half-life of about 1.5 ns. The subsequent gamma transition leads mainly to the ejection of electrons due to internal conversion (IC) and in fewer cases (about 6.63%) to the emission of 35.49 keV gamma-rays. A decay scheme is shown in Figure 1. The atomic relaxation after EC and IC is very complex and various research groups are investigating the ^{125}I decay to get more precise data on the IC process (see, e.g., Tee et al., 2019) or to determine fractional EC probabilities (Kaur et al., 2022).

The Section II of the *Comité Consultatif des Rayonnements Ionisants* (CCRI(II)) organized its most recent international comparison of activity measurements of the same solution of ^{125}I in 2004/2005 and the results were published in 2018 (Ratel, 2018). The participants of the comparison applied various methods such as sum peak counting, various types of 4πβ-γ coincidence or anticoincidence counting, photon-photon coincidence counting, liquid scintillation (LS) counting as well as secondary methods using ionization chambers or calibrated gamma-ray spectrometers (see, e.g., Schrader, 2006; Sahagia et al., 2008; Capogni et al., 2006; Pommé et al., 2005; Ratel, 2018). The comparison showed a rather large spread of the individual results. When considering the final laboratory results of the 22 participants (20 of them applied primary methods), one can find a relative deviation of about 13% between the

highest and lowest results that were obtained for the activity concentration (Ratel, 2018). When excluding the two extreme values, the remaining individual results still scatter in a range of about 6%. Such a scatter is larger than in most CCRI(II) comparisons of other radionuclides and underlines the enormous difficulty of activity measurements of ^{125}I.

It should be noted that the LS methods at the time of the comparison were far less well developed than they are today. In particular the atomic rearrangement models were not detailed enough, and often only a simplified KLM model was adopted which can lead to significant biases (Kossert and Grau Carles, 2008, 2010). Indeed, one participant of the CCRI(II)-K2.I-125(2) comparison who applied the CIEMAT/NIST method can be considered as an outlier. The CIEMAT/NIST method was also applied by the IRMM. However, at that time, they considered this method as "not the most suitable for the standardisation of radionuclides decaying by EC" and thus used six other methods instead (Pommé et al., 2005). The difficulty to measure EC radionuclides with high atomic number is often related to rather high K capture probabilities and a high K fluorescence yield ω_K. The dominance of photon emission leads to a low overall counting efficiency and a larger model dependence when using LS counting (Günther, 2002).

Since the CCRI(II)-K2.I-125(2) comparison was organized almost 20 years ago and since there is a constant demand for activity standards of ^{125}I, LNHB and PTB have decided to conduct a bilateral comparison to probe their measurement capabilities. Both laboratories applied LS methods, and corresponding data were analyzed with independent and more advanced models. In addition, LNHB applied 4π-γ counting (Brinkman and Aten, 1965) for primary activity standardization. Secondary activity standardization methods even allow to establish a link to the latest international comparison. In this way, the quality of the new measurements and, in particular, of the LS methods can be assessed.

2. The ^{125}I solution and general aspects for the comparison

The ^{125}I material used for this comparison was an aqueous carrier free solution obtained from Perkin Elmer and received on 13 January 2021 at LNHB with an activity of about 37 MBq in about 10 uL. In order to ensure the chemical stability of the solution, the drop in the initial vial was mixed and rinsed several times with an ultrapure water solution containing 50 µg $Na_2S_2O_3$ to avoid the formation of the volatile I_2, and 50 µg NaI per gram of solution as carrier. An aliquot of this solution was then diluted using the same chemical mixture to obtain an activity level of about 300 kBq (Ref.: LNHB-125I-19-01-21-B) and then used to fill 5 glass ampoules with weighed aliquots (approximately 5 g each) of the solution and further samples which were measured at LNHB. The glass ampoules were measured in a calibrated ionization chamber at LNHB (see Section 4.3), and then, one of the ampoules with about 5.1 g of the solution was shipped to PTB in February 2021. The participants agreed to use the same reference date, which was defined to be 18 February 2021, 0:00 UTC. Initially, PTB calculated all decay corrections using a half-life of 59.391(18) d taken from Schötzig and Schrader (2000). Later, the participants of the comparison agreed to use a half-life of 59.388(28) d which was taken from Bé et al. (2011). This value was also used for all results stated in this article. However, since all measurements were carried out close to the reference date, the influence of the half-life is relatively small, and the uncertainty of the decay correction is in no case higher than one per thousand.

3. Measurements at PTB

PTB received an ampoule with the identifier LNHB ^{125}I-19-01-21-B; LMRI n°4. Weighed aliquots of the solution were used to prepare LS samples, and two PTB-type flame-sealed glass ampoules with 2 g of solution each. These ampoules were measured in various ionization chambers which are used for secondary standardization. Additional samples were prepared for impurity checks by means of gamma-ray spectrometry. No photon-emitting impurities were found.

Two sets of LS samples were prepared at PTB. The first series was prepared with 15 mL Ultima Gold™ (UG) LS cocktail and about 1 mL of Milli-Q® water (18 MΩ·cm^{-1}) using 20 mL glass vials from Perkin Elmer. The second series was prepared with 15 mL UG and about 0.5 mL of Milli-Q water using 20 mL low diffusion plastic vials from Perkin Elmer. Weighed aliquots of about 20 mg of the radioactive solution were added to the samples using the difference weighing technique. Each sample series comprised 4 radioactive samples plus one compositionally matched background sample. Nitromethane was used as a chemical quenching agent to vary the counting efficiencies in both sample series.

3.1 TDCR measurements

Both LS samples series were measured in a custom-built TDCR counter which was designed at PTB and is referred to as TDCR-M29 (Marganiec-Gałązka et al., 2018). The system makes use of PTB's FPGA-based 4KAM coincidence module (Nähle et al., 2014). The deadtime was adjusted to be 30 µs and it is of an extendable type. The coincidence resolving t_c was adjusted to be 39.5 ns for both sample series. Additional measurements with t_c=199.5 ns were carried out with the samples in PE vials. The experimental coincidence counting rates from the TDCR measurements of the background and the ^{125}I samples were corrected for accidental coincidences (Dutsov et al., 2020).

The analysis was carried out applying a two-step process which comprises the efficiency computations on the basis of an extended stochastic model (Grau Carles, 2007; Kossert and Grau Carles, 2010) plus the analysis of the measurement data with a minimization algorithm to take asymmetries of the photomultiplier (PMT) responses into account (Kossert et al., 2020). For the ^{125}I measurements in TDCR-M29 the asymmetry correction was found to be about -0.35% which is by no means negligible.

The nuclear and atomic input data which are required for the efficiency computation were taken from various sources. The general decay scheme was taken from Bé et al. (2011). It was, however assumed that the gamma/IC transition occurs promptly after the EC decay. Even the smallest coincidence resolving time of 39.5 ns is significantly larger than the half-life of the excited 35.5 keV Te level of about 1.48 ns (Bé et al., 2011), and thus, the gamma/IC transition can be considered as being in coincidence with the EC decay. The fractional EC probabilities were calculated with the BetaShape program (Version: 2.2, May 2021) from Mougeot (2018, 2019, 2021) using a transition energy Q^+= 185.77 keV from the AME2020 evaluation (Wang et al., 2021) and a level energy of 35.49 keV from Bé et al. (2011). The fractional EC probabilities were found to be P_K=0.79927(41), P_{L1}= 0.15171(16) and P_{L2}=0.003908(12). The probability for EC from other shells (M and higher) is calculated as $P_{M+} = 1-P_K- P_{L1}- P_{L2}$. The IC coefficients for the γ transition were calculated with the conversion coefficient calculator BrIcc (v2.3S) using the "frozen orbital" approximation (Kibédi et al., 2008). The K fluorescence yield ω_K=0.875(4) was taken from Bé et al. (2011). Further atomic data were determined with methods and from sources as described by Kossert and Grau Carles (2008). The ionization quenching function $Q(E)$ was calculated using the method described in a previous article (Kossert and Grau Carles, 2010), taking into account the respective composition of the used LS cocktail according to Tan and Xia (2012). The *kB* parameter was chosen to be 75 µm/MeV.

Figure 2 shows the computed double counting efficiency as a function of the TDCR parameter for various configurations. The curves were computed with different *kB* parameters (75 µm/MeV and 110 µm/MeV), for different LS sample compositions (15 mL UG + 1 mL H_2O and 15 mL UG + 0.5 mL H_2O) and assuming different values for the K fluorescence yield (ω_K=0.875 and ω_K=0.883), respectively. The curves show that changes in model assumptions, the assumed sample composition or certain input data can have a very large impact on the efficiency associated with a particular TDCR value. However, the influences are significantly

smaller at high TDCR values, which is why only results from samples with TDCR values greater than 0.76 (corresponds to $\varepsilon_D > 0.89$) were used for the final result.

The determined activity concentration was found to be about 0.7% lower when considering glass vials rather the optical diffusive PE vials. In the following, only results from PE vials are considered as it is recommended to use vials with optical diffusive surfaces when measuring radionuclides with low-energy emissions (see., e.g., Thiam et al., 2012; Broda et al., 2021).

The remaining individual results are illustrated in Figure 3. The figure shows the determined activity concentration as a function of the counting efficiency ε_D. The influence of the coincidence resolving time was found to be very small. However, there is a little trend in the data which indicates that the applied model is still insufficient and/or the nuclear and atomic input data are not correct. Other uncertainty components were evaluated as proposed by Kossert et al. (2015) and an uncertainty budget is shown in Table 1.

3.2 Secondary LS measurements and CIEMAT/NIST efficiency tracing

The LS samples were also measured in a Wallac 1414 Guardian™ liquid scintillation counter and a TriCarb 2800 TR counter from Perkin Elmer. Measured ^{125}I LS spectra of these two instruments are shown in Figure 4 and have the same shape as obtained in several previous ^{125}I measurements carried out at PTB. Thus, there is no evidence of a potential radioactive impurity.

In addition to the ^{125}I measurements, corresponding ^{3}H measurements were also carried out with the same LS sample compositions. In this way, an LS method for secondary activity standardization could be applied as described by Kossert (2006). The efficiency curve $\varepsilon(^{125}\mathrm{I})$ vs. $\varepsilon(^{3}\mathrm{H})$ was derived from experimental data using a ^{125}I solution which was calibrated by photon-photon coincidence counting and can be traced back to the recent CCRI(II)-K2.I-125(2) comparison (Schrader and Walz, 1987; Schrader, 2006; Ratel, 2018). Thus, one can use the secondary LS measurements to establish a link to the key comparison reference value (KCRV)

of the CCRI(II) comparison. It should be noted that the secondary LS method could only be applied with samples in glass vials and a composition with 15 mL UG and 1 mL of water, since the same sample composition was used when establishing the efficiency curve.

The LS measurements in the commercial counters were also analyzed applying the CIEMAT/NIST efficiency tracing (CNET) method. The counting efficiencies were computed with the same approach as for the TDCR method. The determined activity concentration was found to about 1% lower than that obtained from the TDCR measurements at PTB. However, the model dependence is much higher when applying the CNET method. For example, the influence of the *kB* parameter is very large, and also the dependence on the nuclear and atomic data used is significantly larger than with the TDCR method. In addition, one has to account an uncertainty assigned to the ^{3}H activity. The overall relative standard uncertainty was estimated to be 1.9% for the CNET method and PTB decided not to take the result further into account.

3.3 IC measurements

Flame-sealed PTB-type glass ampoules with weighed portions of about 2 g of the radioactive solution were used for measurements in two different ionization chambers. At PTB, such measurements are combined with corresponding measurements of ^{226}Ra reference sources to compensate any long-term stability of the system. One chamber was purchased several years ago from the company MED (Dresden, Germany) and is of type ISOMED 630025, Vacutec 70129. In the following, this chamber is denoted as “ME3”. The second chamber is a Curiementor from PTW (Freiburg, Germany) and will be denoted as “IC5”. Both chambers have thin entrance windows which make them suitable for measurements of radionuclides with emission of low-energy photons. The corresponding calibration factors for ^{125}I can be traced back to photon -photon coincidence counting (Schrader and Walz, 1987; Schrader, 2006). Since

one of the ionization chambers was also used to measure the ^{125}I solution of the most recent CCRI(II)-K2.I-125(2) comparison, it is possible to establish a further link to the KCRV.

4. Measurements at LNHB

One aliquot of the ^{125}I solution was measured by means of gamma-ray spectrometry using an HPGe detector at LNHB. No photon-emitting impurities were detected above the detection limit. In the following, the methods for activity determination are described in detail.

4.1 TDCR measurements

Six LS samples were prepared with the ^{125}I solution using 15 mL UG scintillator in 20-mL PE-PTFE vials. No water or chemical quenching agent was added. The measurements were carried out in a counter system which is referred to as the μTDCR and is shown in Figure 5. The system consists of a very compact 3D-printed chamber and the measurement data was taken using the nano-TDCR module (nanoTDCR, 2019). Details about the counter system can be found elsewhere (Sabot et al., 2022). The extendable deadtime was selected to be 50 μs. The data were recorded simultaneously using two different coincidence resolving times: 40 ns and 400 ns. The influence of the resolving time to the final result was found to be lower than 0.1%. The LS counting efficiency was computed with a program developed at LNHB. The fractional EC probabilities were taken from BetaShape V2.2 (Mougeot, 2019) and further particle and photon emissions were then computed with SASINUC taking into account evaluated DDEP data (Bé et al., 2011). For photons (gamma-rays and x-rays) the resulting electron spectrum was computed using Penelope-based (Salvat, 2019) Monte-Carlo simulations which take the sample composition and geometry into account. The experimental data were corrected for accidental coincidences (Dutsov et al., 2021), and background. The results of the six individual samples were found to be in very good agreement with a relative standard deviation of 0.25%. A detailed

uncertainty budget is shown in Table 2 and the overall relative standard uncertainty was found to be 0.66%.

Additional TDCR measurements were carried out in a system referred to as "RCTD1" which is equipped with three Burle 8850 PMTs and the MAC3 coincidence module (Bouchard and Cassette, 2000). When measuring ^{125}I, the maximum experimental TDCR value was found to be about 0.735 which is much lower than the TDCR ≈ 0.78 value obtained with the μTDCR system. The lower TDCR parameter corresponds to a lower counting efficiency and higher model dependence. Thus, the results obtained from the RCTD1 counter were not used in this work. The findings are similar to the findings from PTB who did not use results of quenched LS samples with lower efficiency for the same reasons.

The analysis of the experimental data was also carried with an additional computation method based on the stochastic approach as described by Kossert and Grau Carles (2010) and using Monte Carlo Geant4 simulations (Agostinelli et al., 2003) for the energies released in the LS cocktail. Decay emission following ^{125}I disintegration including atomic rearrangement was given by the PENNUC package (García-Toraño et al., 2017). As a first step of the analysis, PENNUC was used to simulate random decay pathways of ^{125}I using nuclear decay data provided by the NUCLEIDE database (exported in a specific input file format). For each event generated in a disintegration, the type and energy of emitted particles (e^-, gamma and x-ray) are determined randomly using the decay parameters and branching ratios provided. The atomic relaxation, subsequent to the EC and IC processes leaving to a vacancy in an inner electron sub-shell of the atom, is processed using an energy threshold equal to 50 eV. The information for emitted particles are then stored in an output file event by event and for a given number of disintegrations to be simulated. In a second step, this file containing the coincident particles cascades was loaded in a Geant4-TDCR benchmark developed at LNHB (Thiam et al, 2012) and used as primaries events in order to perform a microscopic simulation of the passage of

each particle through the different elements the TDCR counter (scintillator, vial, optical chamber etc.). Each history is managed as a random sequence of steps in which the particle can interact with the medium. At the end of each event, the energy deposited by the each particle of cascade in the LS volume is collected and stored in a specific output file that also includes the corresponding event number, type of particle, age of particle, position of the emission in the LS-vial and the initial emitted energy. The Birks formula (Birks, 1952) was subsequently applied to each simulated deposited energy recorded in the Monte Carlo output file to take into account ionization quenching for *kB* values ranging from 0.007 to 0.013 cm/MeV. A new output file is then build to include the summation of attenuated energies for each disintegration and for each *kB* values. This new output file (corresponding to 10^6 disintegrations) was then used for the calculation of the detection efficiency of double coincidences based on the formalism of the stochastic approach given by Kossert and Grau Carles (2010). The PMT asymmetry is considered by using three free parameters in the minimization procedure (Broda et al., 2007). The variability of the stochastic approach was optimized by means of the Boostrap technique. The stochastic approach based on Geant4 simulations was applied on the experimental data obtained with the μTDCR device mentioned above. For each source measurement, the calculation of the detection efficiency is based on 10 different sets of $300 \cdot 10^3$ samples randomly drawn with replacement in the total of 10^6 simulated disintegrations and by taking the mean of the 10 results. The activity concentration for each source was finally assessed using the mean of the results obtained with the *kB* values ranging from 0.007 to 0.013 cm/MeV. The activity concentration of the master solution of ^{125}I obtained with the stochastic approach based on Geant4 simulations is equal to 205.2 (13) kBq/g at the reference date. The associated uncertainty budget is given in Table 3.

4.2 4πγ-counting

A cylindrical NaI detector with a diameter of 152 mm and a height of 127 mm with a coaxial re-entrant hole of 21 mm diameter and 47.5 mm height was used for 4πγ-counting. The crystal is coupled to a 9791 type EMI photomultiplier and the assembly is located in a shielding with an internal 1-cm-thick layer of copper and an external 15-cm-thick layer of lead to reduce the background. The pre-amplified signal is filtered and amplified before being processed by a MTR2 discrimination module based on extendable dead-times and the live-time technique (Bouchard, 2000). The pulses of events which are accepted by the MTR2 logic feed an ADC module and the recorded energy histogram is used to estimate the correction with an extrapolation to zero-energy. Finally, the MTR2 is connected to a dual counter/timer to count the detected decay events and to measure the live time using a 1-MHz-frequency clock.

Nine radioactive sources were prepared by dropping weighed aliquots of about 10 mg to 30 mg of the ^{125}I solution (Ref.: LNHB-^{125}I-19-01-21-B LMRI n°5) on top of a 18-µm-thick layer of Mylar sheet using the pycnometer technique. To avoid any loss of the radioactive material, all the iodine was precipitated using a concentrated solution of AgNO3, to form AgI (Lépy, 2016), before the deposit was left to dry in a 60 °C ventilated chamber. Last, a layer of a heat-sealable PET film with a thickness of 70 µm was used to seal the sources, before a punch-cutting step. The diameter of assembly disks is 18 mm , which is adapted for the detector re-entrant hole.

The detection efficiency was calculated using the Geant4 code (Agostinelli et al., 2003) based on a comprehensive modelling of the detection system. The calculated detection efficiency was 0.915 (5). The correction for the zero-energy extrapolation is applied to compensate for counting losses below the detection threshold, which is set at a level slightly above the electronic noise (~ 10 keV for ^{125}I measurements). The correction 1.0002 (1) is estimated using a conservative calculation (Thiam et al., 2015). The results of the nine individual sources were

in excellent agreement (standard deviation of 0.1%). A detailed uncertainty budget is shown in Table 4 and the overall relative standard uncertainty was found to be 0.51%.

4.3 IC measurements

Five "LMRI" glass sealed ampoules (wall thickness: 0.61 (1) mm) filled with 5 mL of ^{125}I were measured using a Vinten 671 ionization chamber (referred as to "2A"), which is similar to the IG42 IC constructed by Centronic. This chamber has an aluminum alloy re-entrant well and electrode (both 2 mm thick), and has an effective volume of 10.5 L filled with nitrogen at a pressure of about 1 MPa. A 50-mm thick low-activity lead shield surrounds the chamber in order to reduce the ambient background and prevent any efficiency variations caused by scattering in the surrounding materials (the mean background current measured is 20 fA). A 6517 Keithley electrometer is used to supply the high voltage, as well as measure collected charges via an interface bus (GPIB). A homemade program controls the activity measurement, current calculations, background and decays corrections. The whole measurement system stability is checked using long period source.

The calibration factor of ionization chamber "2A" for the 5 mL-ampoule was obtained from primary standard measurement using TDCR method (Ratel et al, 1988).

The activity concentration of the master solution of ^{125}I at the reference date, 208.1 (9) kBq/g, was obtained from mean value of three ampoules out of the 5 measured.

5. Comparison of results and conclusions

The results of the individual measurements at PTB and LNHB are summarized in Table 5 and illustrated in Figure 6. All results are in a rather good agreement. In particular, the results from the primary activity measurements (TDCR and 4πγ-counting) are very close. The highest activity concentration is obtained from the ionization chamber measurement at LNHB, but it

still agrees within one standard uncertainty with most other results. All secondary standardization results from PTB agree well, which was expected as they can be traced back to the same reference method. The corresponding results were used to establish a link to the KCRV of the CCRI(II)-K2.I-125(2) comparison. For the sake of simplicity, we omit a detailed discussion of uncertainty here.

In conclusion, the results of the two laboratories are in very good agreement. The indirect comparison also shows that the results of the primary methods are consistent with the KCRV of the CCRI(II)-K2.I-125(2). This underlines that significant progress has been made, especially in the TDCR method. The results from primary activity standardization in this work make it possible to evaluate new calibration factors for the ionization chambers which are usually the workhorses for routine activity determinations in metrology institutes.

However, despite the progress achieved in this work, ^{125}I is still considered to be a very difficult radionuclide to measure. The situation is partly exacerbated by the fact that some established standardisation methods, like photon-photon coincidence counting, can no longer be applied due to the unavailability of appropriate equipment and expertise. A wide variety of measurement methods is therefore helpful and from time to time international comparisons should also be organised with as many participants as possible.

Acknowledgements

We wish to thank the gamma-ray spectrometry team from PTB for the impurity checks. The authors are indebted to Xavier Mougeot for the help of the BetaShape and SAISINUC calculations which were used for the TDCR analysis at LNHB.

References

Agostinelli, S., et al., 2003. Geant4 – a simulation toolkit. Nucl. Instrum. Meth. A 506, 250–303.

Bé M.-M., Chisté V., Dulieu C., Mougeot X., Chechev V., Kuzmenko N., Kondev F., Luca A., Galán M., Nichols A.L., Arinc A., Pearce A., Huang X., Wang B., 2011, Monographie BIPM-5: Table of radionuclides, Vol. 6.

Birks, J.B., 1952. Theory of the response of organic scintillation crystals to short-range particles. Phys. Rev. 86, 56.

Bouchard, J., 2000. MTR2: a discriminator and dead-time module used in counting systems. Appl. Radiat. Isot. 52, 441-446.

Bouchard, J., Cassette, Ph., 2000. MAC3: an electronic module for the processing of pulses delivered by a three photomultiplier liquid scintillation counting system. Appl. Radiat. Isot. 52, 669-672.

Brinkman, G. A., Aten, A. H. W. Jr., 1965. Absolute standardization with a NaI(Tl) crystal – V. Calibration of isotopes with complex decay schemes. Int. J. Appl. Radiat. Isot. 16 177-181.

Broda, R., Cassette, P., Kossert, K., 2007. Radionuclide metrology using liquid scintillation counting. Metrologia 44, S36-S52.

Broda, R. , Bonková, I., Capogni, M., Carconi, P., Cassette, P., Coulon, R., Courte, S., De Felice, P., Dziel, T., Fazio, A., Frechou, C., Galea, R., García-Toraño, E., Kołakowska1, E., Kossert, K., Krivošík, M., Lech, E., Lee, K.B., Liang, J., Listkowska, A., Liu, H., Navarro, N., Nähle, O.J., Nowicka, M., van Rooy, M., Sabot, B., Saganowski, P., Sato, Y., Tymiński, Z., Yunoki, A., Zhang, M., Ziemek, T., 2021. The CCRI(II)-K2.Fe-55.2019 key comparison of activity concentration measurements of a ^{55}Fe solution. Metrologia 58, 1A Techn. Suppl., 06010.

Capogni, M., Ceccatelli, A., De Felice, P., Fazio, A., 2006. Random-summing correction and pile-up rejection in the sum-peak method. Appl. Radiat. Isot. 64, 1229-1233.

Dutsov, Ch. Cassette, Ph., Sabot, B., Mitev, K., 2020. Evaluation of the accidental coincidence counting rates in TDCR counting. Nucl. Instrum. Meth. A 977, 164292.

García-Toraño, E., Peyres, V., Bé, M.-M., Dulieu, C., Lépy, M.-C., Salvat F., 2017. Simulation of decay processes and radiation transport times in radioactivity measurements. Nucl. Instrum. Meth. B 396, 43-49.

Grau Carles, A., 2007. MICELLE, the micelle size effect on the LS counting efficiency. Comput. Phys. Commun. 176, 305-317.

Günther E., 2002. What can we expect from the CIEMAT/NIST method? Appl. Radiat. Isot. 56, 357–360.

Huang, G., 2019. Nuclear medicine in oncology - Molecular imaging and target therapy. Springer Nature Singapore. https://doi.org/10.1007/978-981-13-7458-6.

Kaur A., Loidl, M., Rodrigues, M., 2022. Determination of fractional electron capture probabilities of ^{125}I using metallic magnetic calorimeters. J. Low Temp. Phys. 209, 864–871.

Kibédi, T., Burrows, T.W., Trzhaskovskaya, M.B., Davidson, P.M., Nestor, C.W. (Jr.), 2008. Evaluation of theoretical conversion coefficients using BrIcc. Nucl. Instrum. Meth. A 589, 202-229. And: http://bricc.anu.edu.au/ (accessed January 2019).

Kossert, K., 2006. A new method for secondary standard measurements with the aid of liquid scintillation counting. Appl. Radiat. Isot. 64, 1459-1464.

Kossert, K., Grau Carles, A., 2008. Study of a Monte Carlo rearrangement model for the activity determination of electron-capture nuclides by means of liquid scintillation counting. Appl. Radiat. Isot. 66, 998-1005.

Kossert, K., Grau Carles, A., 2010. Improved method for the calculation of the counting efficiency of electron-capture nuclides in liquid scintillation samples. Appl. Radiat. Isot. 68, 1482-1488.

Kossert, K., Broda, R., Cassette, Ph., Ratel, G., Zimmerman, B., 2015. Uncertainty determination for activity measurements by means of the TDCR method and the CIEMAT/NIST efficiency tracing technique. Metrologia 52, S172-S190 (Special Issue on Uncertainty Evaluation in Radionuclide Metrology).

Kossert, K., Sabot, B., Cassette, P., Coulon, R., Liu, H., 2020. On the photomultiplier-tube asymmetry in TDCR systems. Appl. Radiat. Isot. 163, 109223.

Lépy, M.-C., Brondeau, L., Bobin, C., Lourenço, V., Thiam, C., Bé, M.-M., 2016. Determination of X- and gamma-ray emission intensities in the decay of ^{131}I, Appl. Radiat. Isot. 109, 154-159.

Marganiec-Gałązka, J., Nähle, O.J., Kossert, K., 2018. Activity determination of ^{68}Ge/^{68}Ga by means of 4π(Č)β-γ coincidence counting, Appl. Radiat. Isot. 134, 240-244.

Mougeot, X., 2018. Improved calculations of electron capture transitions for decay data and radionuclide metrology. Appl. Radiat. Isot. 134, 225-232.

Mougeot, X., 2019. Towards high-precision calculation of electron capture decays. Appl. Radiat. Isot. 154, 108884.

Mougeot, X., 2021. BetaShape – v2.2, http://www.lnhb.fr/rd-activities/spectrum-processing-software/, website accessed: 21 July 2021.

Nähle, O., Zhao, Q., Wanke, C., Weierganz, M., Kossert, K., 2014. A portable TDCR system. Appl. Radiat. Isot. 87, 249-253.

nanoTDCR 2019. nanoTDCR - Triple-to-Double Coincidence Ratio Liquid Scintillation Counting System (TDCR) and MCA. Data Sheet, Labzy/Yantel, https://www.yantel.com/wp-content/uploads/nanoTDCR_TD9009_TD9010_Data_Sheet_Rev_01Cs.pdf (page accessed 6 March 2023).

Pommé, S., Altzitzoglou, T., Van Ammel, R., Siggens, G., 2005. Standardisation of ^{125}I using

seven techniques for radioactivity measurement. Nucl. Instrum. Meth. A 544, 584-592.

Ratel, G., 2018. International comparison of activity measurements of a solution of ^{125}I. Report available at https://www.bipm.org/kcdb/ with identifier CCRI(II)-K2.I-125(2).

Ratel G., Mtiller, J.W., 1988. Trial comparison of activity measurements of a solution of ^{125}I, final report, Rapport BIPM-88/2, 22 pages. (Bureau International des Poids et Mesures. F-92312 Sevres Cedex, 1988).

Sabot, B., Dutsov, C., Cassette P., Mitev, K., 2022. Performance of portable TDCR systems developed at LNE-LNHB, Nucl. Instrum. Meth. A 1034, 166721, https://doi.org/10.1016/j.nima.2022.166721.

Sahagia, M., Ivan, C., Grigorescu, E.L., Razdolescu, A.C., 2008. Standardization of ^{125}I by the coincidence method and practical applications. Appl. Radiat Isot. 66, 895-899.

Salvat, F., 2019. PENELOPE-2018: A Code System for Monte Carlo Simulation of Electron and Photon Transport, NEA/MBDAV/R1, https://doi.org/10.1787/32da5043-en.

Schötzig, U., Schrader, H., 2000. Halbwertszeiten und Photonen-Emissionswahrscheinlichkeiten von häufig verwendeten Radionukliden. PTB report PTB-Ra-16/5, ISBN 3-89701-279-0.

Schrader, H., Walz K.F., 1987. Standardization of ^{125}I by Photon-Photon Coincidence Counting and Efficiency Extrapolation. Appl. Radiat Isot. 38, 763-766.

Schrader, H., 2006. Photon-photon coincidences for activity determination: I-125 and other radionuclides. Appl. Radiat Isot. 64, 1179-1185.

Tan, Z., Xia, Y., 2012. Stopping power and mean free path for low-energy electrons in ten scintillators over energy range of 20–20,000 eV. Appl. Radiat. Isot. 70, 296–300.

Tee, B.P.E, Stuckberry, A.E., Vos, M., Dowie, J.T.H., Lee, B.Q., Alotiby, M., Greguric, I.,

Kibédi, T., High-resolution conversion electron spectroscopy of the ^{125}I electron-capture decay. Phys. Rev. C 100, 034313.

Thiam, C., Bobin, C., Chauvenet, B., Bouchard, J., 2012. Application of TDCR-Geant4 modeling to standardization of ^{63}Ni.Appl. Radiat. Isot. 70, 2195-2199.

Thiam, C., Bobin, C., Maringer, F.J., Peyres, V., and Pommé, S., 2015. Assessment of the uncertainty budget associated with 4πγ counting. Metrologia 52 S97–S107.

Wang, M., Audi, G., Kondev, F.G., Huang, W.J., Naimi, S., Xu, X., 2017. The AME2016 atomic mass evaluation (II). Chinese Phys. C 41, 03003.

Wei, S., Li, C., Li, M., Xiong, Y., Jiang, Y., Sun, H., Qiu, B., Lin, C.J., Wang, J., 2021. Radioactive iodine-125 in tumor therapy: Advances and future directions. Frontiers in Oncology 11, 717180, 1-24.

Table 1

Uncertainty budget (k=1) for the activity concentration a determined by means of TDCR at PTB.

Uncertainty component	$u(a)/a$ **in %**
Counting statistics	0.14
Weighing	0.04
Dead time	0.05
Background	0.03
Adsorption	0.05
TDCR value	0.1
Sample (in)stability	0.15
Model	0.4
Impurities	0.03
Ionization quenching	0.2
Decay data (fractional EC probabilities, ω_K, etc.)	0.4
PMT asymmetry	0.03
Decay correction	0.03
Combined uncertainty	**0.65**

Table 2

Uncertainty budget (k=1) for the activity concentration a determined by means of TDCR at LNHB.

Uncertainty component	$u(a)/a$ **in %**
Counting statistics	0.05
Dispersion (relative standard deviation of six LS samples)	0.25
Live time	0.02
Decay correction	0.03
Nuclear data + Monte Carlo	0.60
kB parameter	0.10
Background	0.10
Accidental coincidences	0.01
Combined uncertainty	**0.66**

Table 3

Uncertainty budget (k=1) for the activity concentration a obtained with the stochastic approach based on Geant4 simulations applied on experimental data given by the μ-TDCR device at LNHB.

Uncertainty component	$u(a)/a$ **in %**
Variability on the measurements of 6 LS sources	0.22
Active time	0.02
Weighing	0.05
Decay correction	0.03
TDCR model including nuclear data / Monte Carlo simulations	0.58
kB parameter (variability between 0.007 cm/MeV to 0.013 cm/MeV)	0.04
Background	0.10
Accidental coincidences	0.01
Relative combined uncertainty	**0.63**

Table 4

Uncertainty budget (k=1) for the activity concentration a determined by means of 4πγ-counting at LNHB.

Uncertainty component	$u(a)/a$ **in %**
Counting statistics	0.10
Background	0.10
Weighing	0.05
Dead time	0.01
Decay correction	0.10
Zero energy extrapolation	0.10
Detection efficiency	0.50
Combined uncertainty	**0.51**

Table 5

Activity concentration of the ^{125}I solution studied in this work for various individual methods (reference date: 18 February 2021, 0.00 UTC). The uncertainties correspond to standard uncertainties (k=1).

	a **in kBq/g**	$u(a)$ **in kBq/g**
LNHB-TDCR	204.7	1.4
LNHB-4π-γ	204.8	1.1
LNHB-IC	208.1	0.9
PTB-TDCR	205.4	1.4

PTB-LSC secondary	207.2	2.1
PTB-ME3	205.60	1.74
PTB-IC5	207.39	1.76
PTB-IC (combined)	206.5	1.6

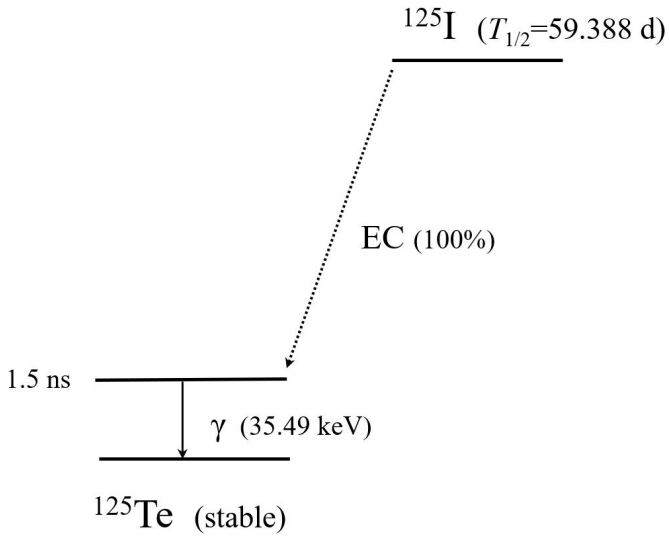

Figure 1: Decay scheme of ^{125}I. Data were taken from Bé et al. (2011).

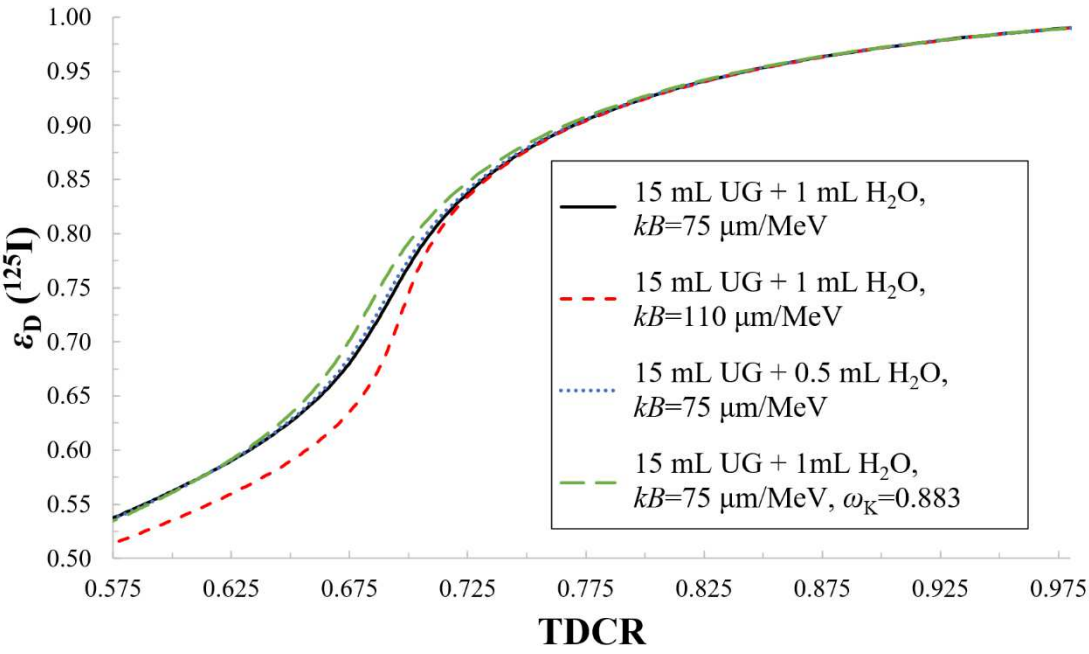

Figure 2: Computed efficiency ε_D for the logical sum of double coincidence as a function of the TDCR parameter. The black solid line was obtained for an LS composition with 15 mL UG and 1 mL H_2O and *kB*=75 µm/MeV while the red dashed line was obtained for the same composition but using *kB*=110 µm/MeV. The other curves were computed for an LS sample composition with 15 mL UG and 0.5 mL H_2O using ω_K=0.875 (blue dotted curve) and ω_K=0.883 (green long-dashed curve).

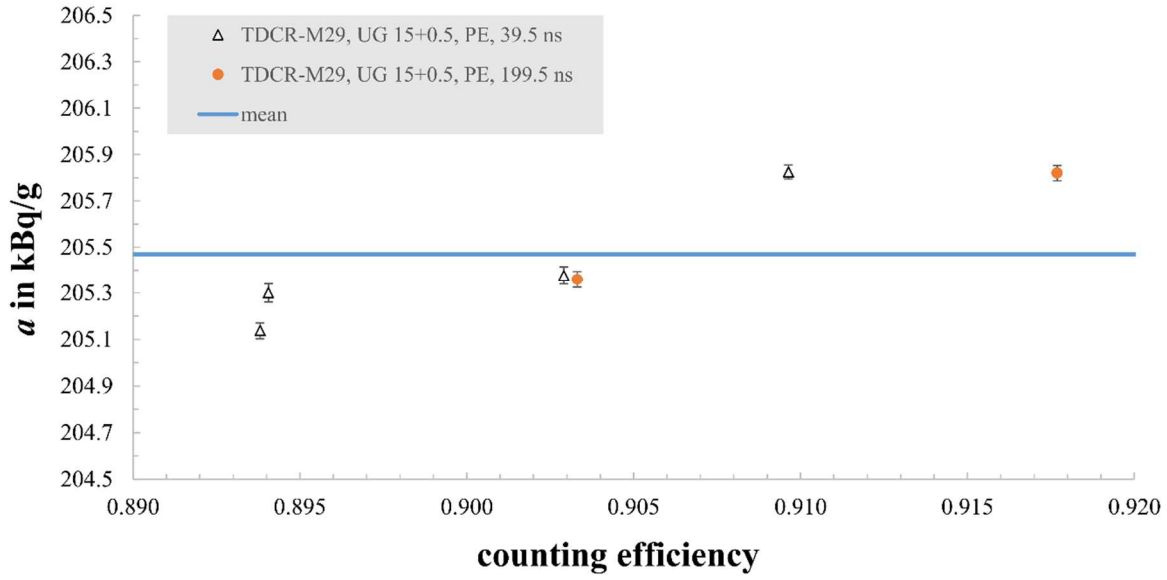

Figure 3: Activity concentration as obtained at PTB for the TDCR method as a function of the counting efficiency ε_D. The uncertainty bars represent only a statistical component calculated as a standard deviation of the mean of several repeat measurements. The figure shows only results of measurements with PE vials and TDCR values larger than 0.76.

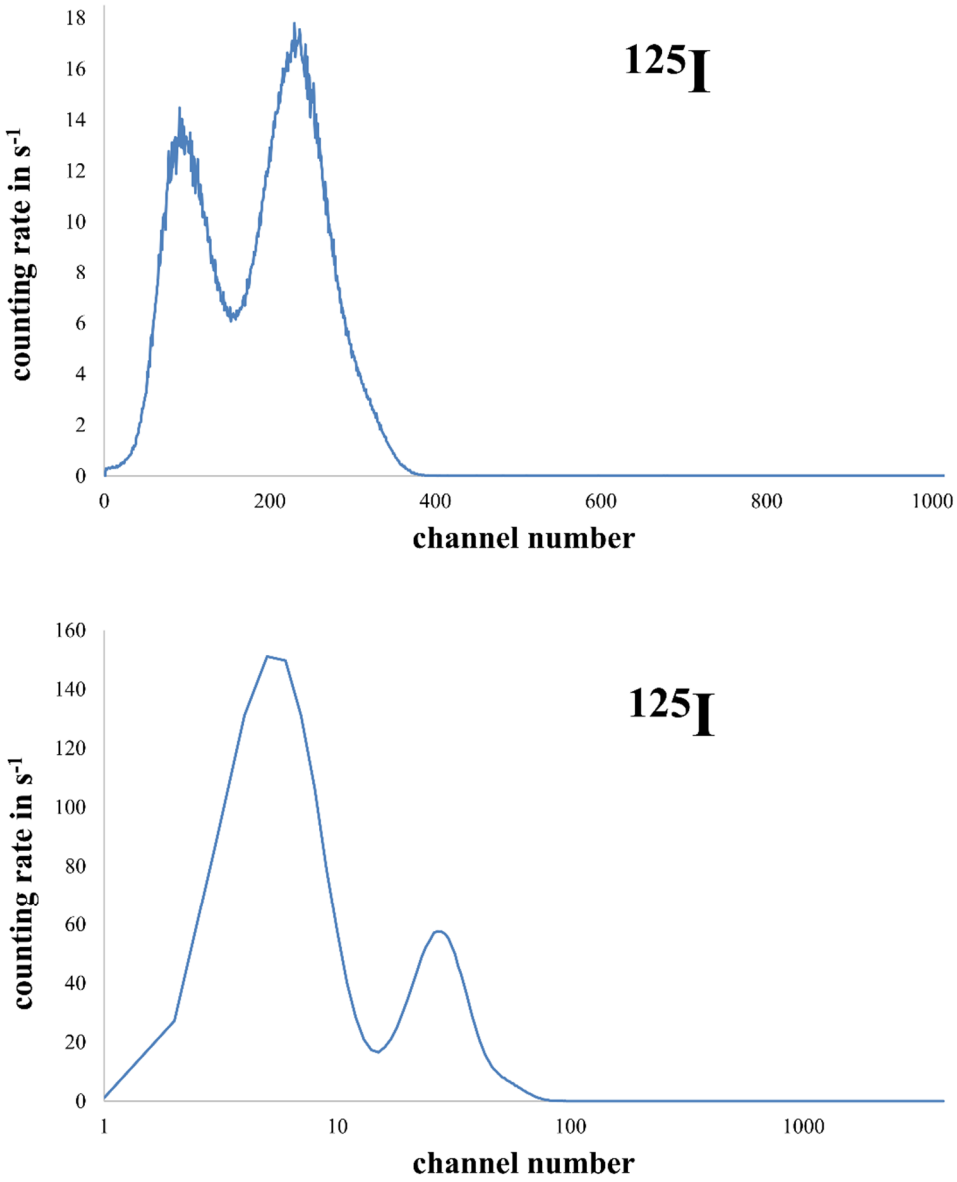

Figure 4: Spectra of ^{125}I LS samples recorded with a Wallac 1414 counter (top) and a TriCarb 2800 TR counter (bottom). Corresponding background spectra have been subtracted.

Figure 5: The µTDCR setup at LNHB with (from right to left) the nanoTDCR module, an LS sample, the 3D-printed detector housing containing the optical chamber and PMTs, a HV power supply and a transport case in the background.

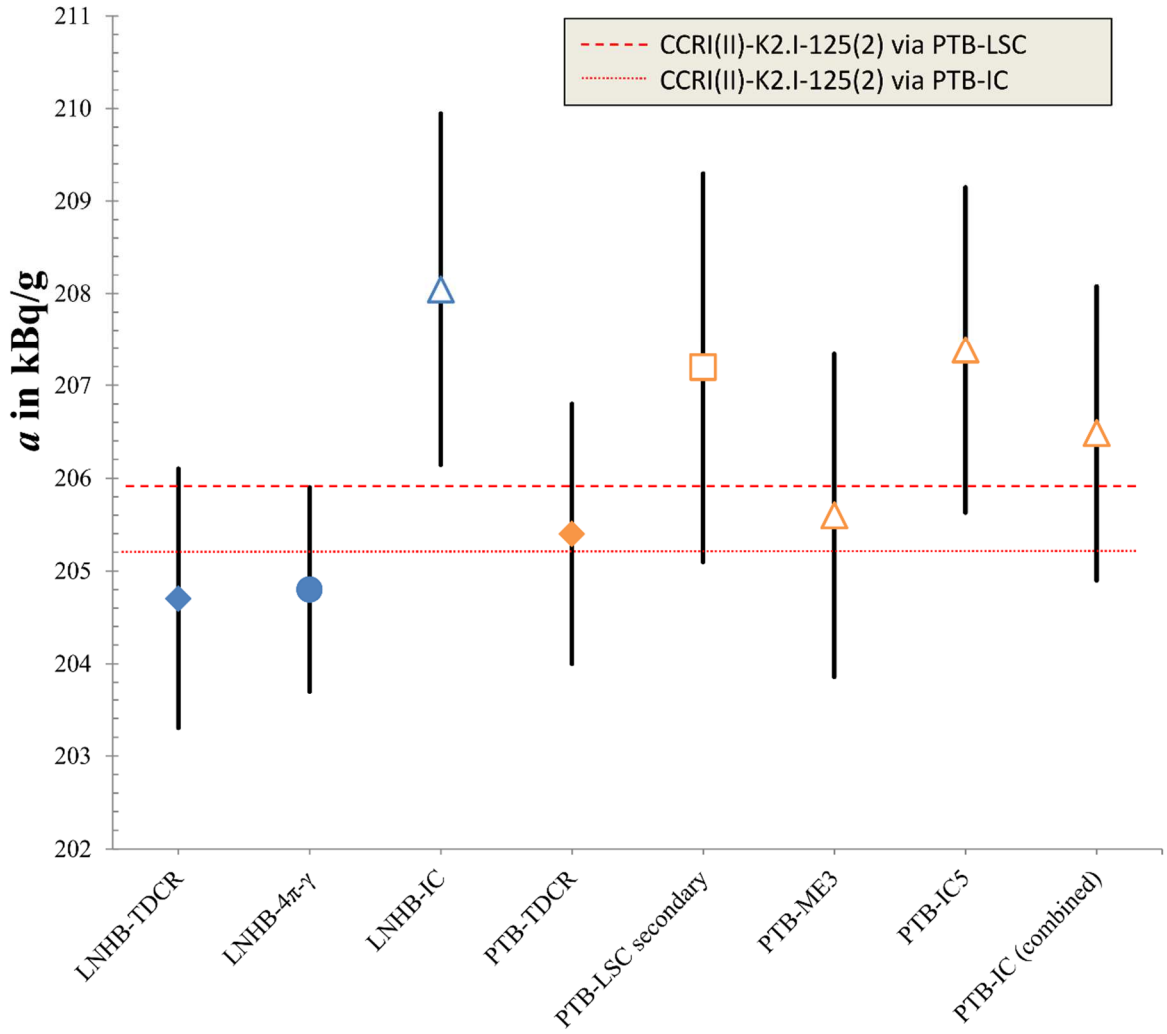

Figure 6: Activity concentration as obtained from various measurement methods applied at LNHB and PTB. Secondary measurement methods (open symbols) of PTB were also used to link the result to the latest CCRI(II) comparison on ^{125}I.